# Computational Lighting by a LED-based System

Ming-Chin Chien and Chung-Hao Tien
Department of Photonics, National Chiao Tung University, 1001 University Road, Hsinchu, Taiwan

## ABSTRACT

A methodology analogous to a general lens design rule was proposed to step-by-step optimize the spectral power distribution (SPD) of a composite light-emitting diodes (LEDs) cluster. The computation is conducted for arbitrary SPD combination for the applications in radiometry, photometry and colorimetry, respectively. Based on the matrix computation, a spectrally tunable source is implemented to strategically manipulate the chromaticity, system efficiency and light quality according to all kinds of operational purposes. By the R/G/B/A/CW light engine with graphic utility interface, the cluster engine was experimentally validated to offer a wide-ranged operation in ambient temperature ($T_a$ = 10°C to 100°C) with high color quality scale (CQS > 85 points) as well as high luminous efficiency (LE > 100 lm/watt) over the chromaticity point from 2800K to 8000K.

**Keywords:** computational lighting, composite LEDs cluster, SPD synthesis

## 1. INTRODUCTION

The progress in LEDs technology has been breathtaking during the last few decades. At this time, great technological advances in solid-state lighting are profoundly changing the way light was generated. Unlike the conventional incandescent or fluorescent sources, LEDs could offer not only the possibly highest optoelectronic conversion efficiency, but also the capability of modulating its composite spectral distribution in accordance with various operational environments and requirements via the cluster configuration [1-2]. Such spectrum-controllable property is probably the most relevant to the emerging intelligent lighting [3-4]. In 2010, A. Žukauskas et al presented a trichromatic cluster composed of red/green/blue single-color LEDs with high color saturation ability [5]. Soon afterwards, G. He and L. Zheng realized a color-tunable hybrid system by one phosphor-based and two single-color LEDs [6]. Previous studies in general provided good guidelines for specific purposes, while the complete treatment for spectral synthesizing was left a space to be addressed. As we considered this topic, we were thinking if there was a unifying theme for composite spectrum engineering in fields of smart lighting, if so, what was it?

To help guide us in the investigation, we begin with a linear transformation, a fundamental operation in fields of digital signal processing, spectroscopic system and optical communication [7-8]. As shown in Fig. 1, a general mixing mechanism is considered as the operation executing a matrix-vector multiplication. The elements of the input vector **k** refer to the weighting ratios for the N source types, which are defined as the ratios of the used drive currents normalized to the maximum available ones. The N weighting signals are multiplexed to a LEDs cluster and projected on the spectral response matrix **R**. Each column of **R** represents a spectral impulse response (**r**) corresponding to one type of LED. For example, element $r_{ij}$ of matrix **R** denotes the spectral value of wavelength $\lambda_{ij}$, which is the $i^{th}$ sampling point of $j^{th}$ source driven under the unit weighting ratio condition. The resultant mixing spectrum **s** of the **R**-**k** multiplication is equivalent to the linear combination of each impulse response, whose value can be detected by the spectroradiometer (SR).

In the ideal assumption, the spectral impulse response (**r**) would be thermal invariant and set as a constant. Since the material nature of the LED device, **r** in practice changes with junction temperature. The challenge in the beginning has been to model the behavior of **R** as close as that for practical use. Our intent in this issue is to regard the single-color spectral response as a superposition of two Gaussian functions and then show how principle features (i.e. intensity, peak wavelength, and spectral width) of Gaussians have changed as the temperature has changed. We show also that the method is likely for phosphor-based LED as long as the fluorescence and the excitation region could be roughly separated.

Ultimately we develop a design procedure of the composite spectrum for functional illuminations. The concept comes up from the conventional lens design techniques. In order to validate the proposed scheme, we take each entry $r_{ij}$ as a platform to carry out the home-made LEDs cluster for a user-defined merit function. The results show that the

Current Developments in Lens Design and Optical Engineering XIII, edited by R. Barry Johnson,
Virendra N. Mahajan, Simon Thibault, Proc. of SPIE Vol. 8486, 84860R

optimal operation points are readily obtained to achieve the balance between color rendering performance and power consumption over the wide range of chromaticity point.

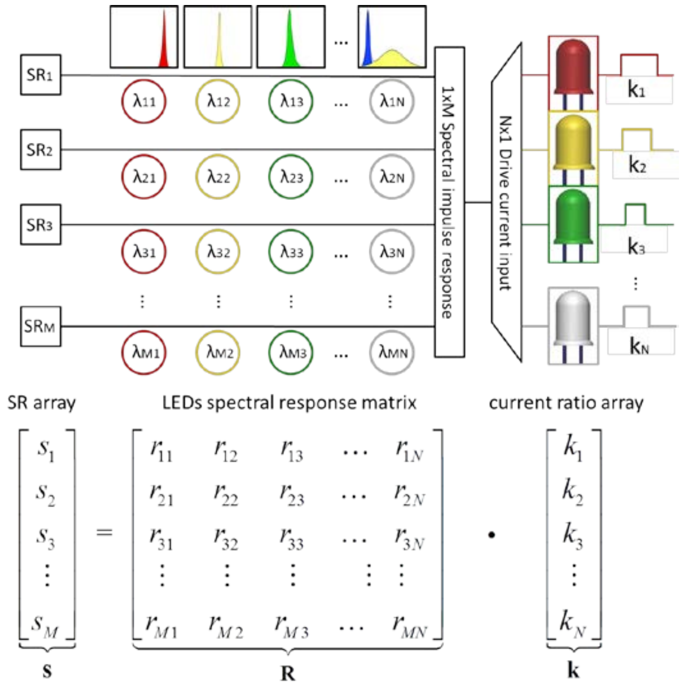


Figure 1 Schematic of the composite spectral engineering, which performs the matrix-vector multiplication of **s** = **R** · **k**. The bold-faced capital letter **R** refers to the matrix of the spectral response, and the bold-faced lower-case letters **k** and **s** denote the vector of weighting ratios for N source types and the vector of resultant mixing spectrum, respectively. SR, spectroradiometer.

## 2. METHODS

### 2.1 LED spectral characterization

In general, the single-color SPD is similar to a Gaussian distribution that can simply be specified by three principle features, i.e. intensity ($p$), peak wavelength ($\hat{\lambda}$) and spectral width ($\Delta\lambda$); Thus, if the spectral impulse response (**r**) is well fitted by the Gaussians, a great dimensional reduction, from N to three, will be made. Typically, a more accuracy model usually employees the double-Gaussian fitting [9-10]. We follow the same route to use the normal double-Gaussian with two sets of parameters: $(p,\ \hat{\lambda},\ \Delta\lambda)$ and $(p',\ \hat{\lambda}',\ \Delta\lambda')$, where all features more or less would have certain relations with junction temperature $T_j$ and DC drive current $I_{DC}$. We empirically estimate the features-temperature and the features-current relations as simple as possible, which can be expressed in matrix form:

$$\ln(\mathbf{p}) = \mathbf{M_p}\mathbf{c_p} \tag{1a}$$

$$\hat{\boldsymbol{\lambda}} = \mathbf{M}_\lambda \mathbf{c}_\lambda \tag{1b}$$

$$\ln(\boldsymbol{\Delta\lambda}) = \mathbf{M}_{\Delta\lambda}\mathbf{c}_{\Delta\lambda} \tag{1c}$$

where $\mathbf{M_p} = [\mathbf{t_j}^{\mathbf{T}} \ln(\mathbf{t_j})\ \ \ln(\mathbf{i_{DC}})\ \ \mathbf{l}]$, $\mathbf{M}_\lambda = [\mathbf{t_j}\ \ \ln(\mathbf{i_{DC}})\ \ \mathbf{l}]$ and $\mathbf{M}_{\Delta\lambda} = [\mathbf{t_j}\ln(\mathbf{t_j})^{-1}\ \ (\mathbf{i_{DC}})^{1/2}\ \ \mathbf{l}]$ are $M$ x 3 basis matrices for **p**, $\hat{\boldsymbol{\lambda}}$ and $\boldsymbol{\Delta\lambda}$, respectively. The term **l** indicates the $M$ x 1 all-ones vector. $\mathbf{c_p}$, $\mathbf{c}_\lambda$, and $\mathbf{c}_{\Delta\lambda}$ refer to 3x1 vectors of fitting coefficients, whose values could be calculated by linear least square method, e.g. the vector of intensity coefficient can be obtained as $\mathbf{c_p} = \left(\mathbf{M_p}^{\mathbf{T}}\mathbf{M_p}\right)^{-1}\mathbf{M_p}^{\mathbf{T}}\ln(\mathbf{p})$. Figure 2(a) shows all element values of intensity **p** and fitting coefficients

$c_{p1}$, $c_{p2}$ and $c_{p3}$ for red AlInGaP LED (HMHP-E1HR). The corresponding goodness of fit in Figure 2(b) reveals that the intensity variance, caused by the changes of temperature and current, can be well estimated by Equation (1a).

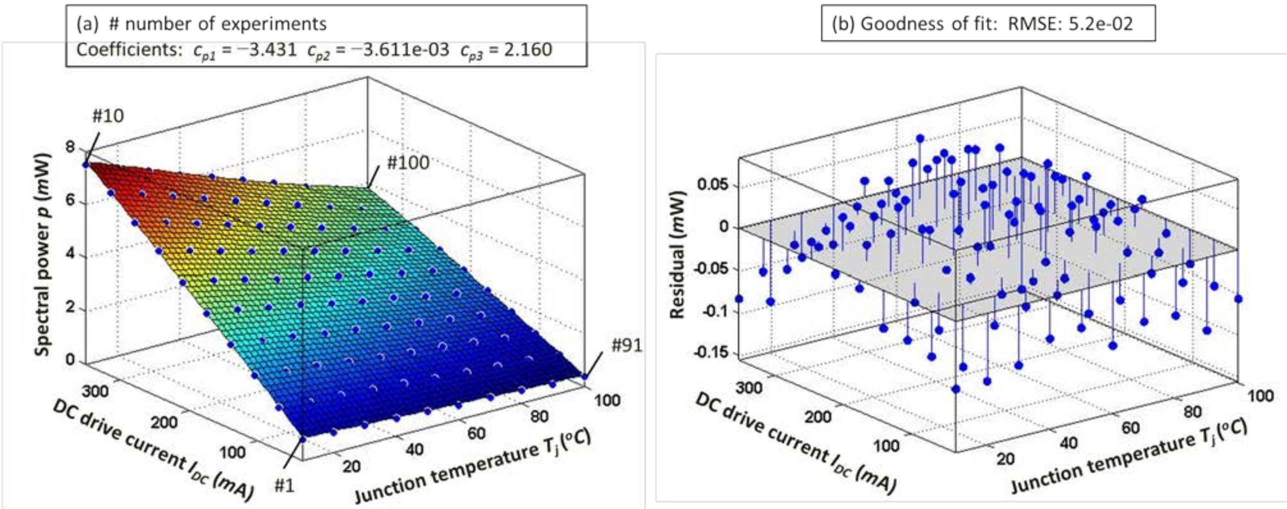


Figure 2. (a) All element values of intensity **p** and fitting coefficients $c_{p1}$, $c_{p2}$ and $c_{p3}$ for red AlInGaP LED (HMHP-E1HR). (b) The corresponding goodness of fit. The results show the root mean square error (RMSE) < 5.2e-02, so that the intensity variance can be well estimated by Equation (1a).

As a consequence, the single-color spectrum $S(\lambda)$ could be well characterized via the recombination of the two normal Gaussians with the appropriate coefficients:

$$\begin{aligned} S(\lambda) = {} & \exp[\mathbf{m_p c_p} - (\lambda - \mathbf{m_\lambda c_\lambda})^2 / \exp(\mathbf{m_{\Delta\lambda} c_{\Delta\lambda}})^2] \\ & + \exp[\mathbf{m_p c_p}' - (\lambda - \mathbf{m_\lambda c_\lambda}')^2 / \exp(\mathbf{m_{\Delta\lambda} c_{\Delta\lambda}}')^2] \end{aligned} \tag{2}$$

where $\mathbf{m_p} = [T_j \ln(T_j) \;\; \ln(I_{DC}) \;\; 1]$, $\mathbf{m_\lambda} = [T_j \;\; \ln(I_{DC}) \;\; 1]$, and $\mathbf{m_{\Delta\lambda}} = [T_j \ln(T_j)^{-1} \;\; (I_{DC})^{1/2} \;\; 1]$ account for basis vectors of the intensity ($P$), peak wavelength ( $\hat{\lambda}$ ) and spectral width ($\Delta\lambda$) with variables $T_j$ and $I_{DC}$.

For the phosphor-converted white LED $S_W(\lambda)$, the spectrum is composed of the excitation and the fluorescence part, whose temperature and current dependences are subject to the innate character of different materials. To model the $S_W(\lambda)$, we define a cutoff wavelength that can roughly separate the excitation spectrum from that of fluorescence region, and then sequentially impose the rules, the same as in the single-color case, to each part.

### 2.2 Optimization process

The solution of lens design is typically an inverse problem. Given the effective focal length (EFL) and degrees of correction for an optical system, it is possible to determine the curvatures, the thicknesses, and the number of lenses accordingly. For example, if we aim to design a lens system with a specified EFL and correct three Seidel aberration coefficients, it can be analytically resolved by a set with two singlet lenses, that leaves four degrees of freedom, two powers and two shape factors [the shape factor is defined as $(R_2 + R_1) / (R_2 - R_1)$, where $R_1$ and $R_2$ are the radii of the first and second surfaces, respectively] [11]. However, due to the complexity of multiple lenses that increases the computational cost, the more efficient method in lens design would resort to an iterative process [12], as shown in Figure 3(a).

In multispectral mixing, the similar optimization issue inspired us to borrow lens design process by replacing the lens system with a LEDs cluster. First of all, we emulate a single-colour LED as a singlet, whose light bending power determined by its curvature and refractive index can be conceptually analogous to the emitting luminous flux of a LED determined by the driving current and luminous efficiency, respectively. As we mix a number of LEDs, the additive mixing by two single-colour LEDs is equivalent to two singlet lenses. Likewise, the LED-plus-phosphor based approach can be regarded as a cemented doublet (dichromatic) or triplet (trichromatic), depending on the number of emitting peak wavelengths. Based on above hypothesis outlined, the SPD synthesis can be transformed into a classic lens design problem. For example, a LED cluster composed of red/cool-white/cool-white/green is logically equivalent to a double Gauss lens system. The diffraction limitation of a lenses system is also viewed as the theoretical boundary of the luminous efficacy of radiance (LER) or color rendering index (CRI) accordingly. The corresponding design procedure is proposed in Figure 3(b).

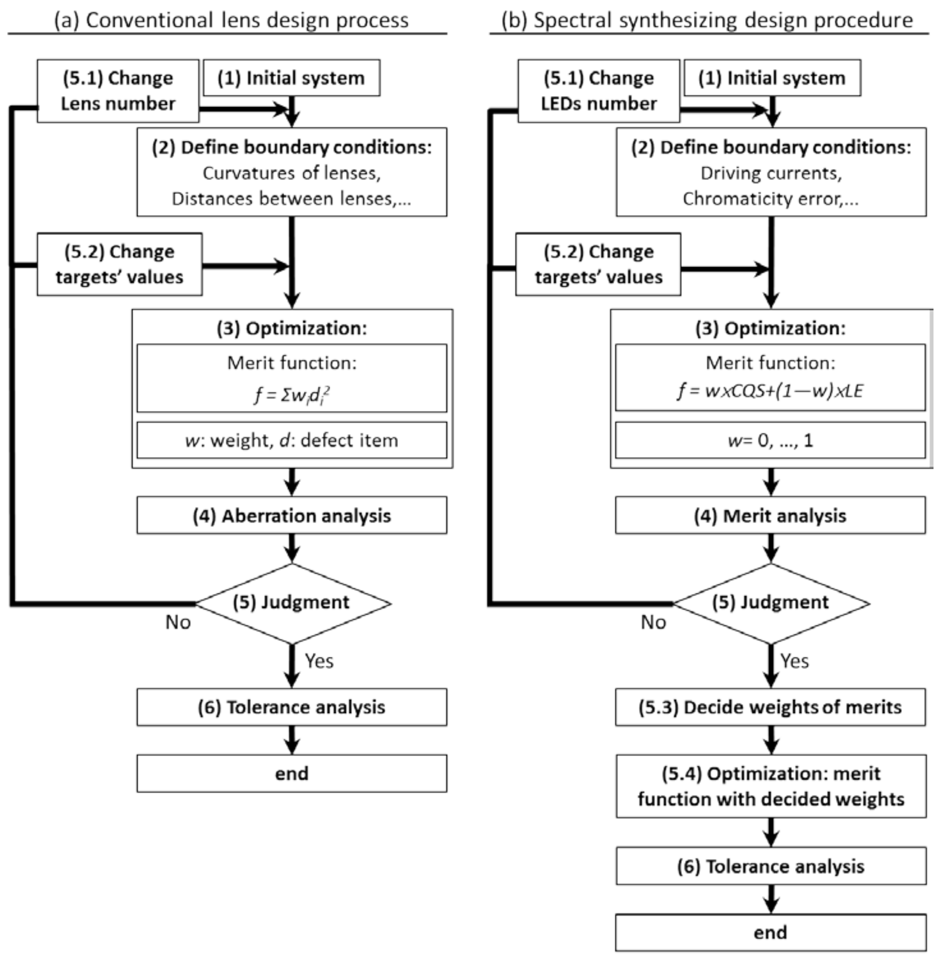


Figure 3 Design procedure of (a) lens design and (b) spectral synthesis of a LEDs cluster. Both flow charts include six steps: (1) initial system, (2) define boundary condition, (3) optimization, (4) aberration or merit analysis, (5) judgment, and (6) tolerance analysis.

## 3. DESIGN EXAMPLE

In this section, we verify the proposed scheme efficient in spectral mixing design by implementing a pendachromatic high power LEDs cluster for general lighting use. Figure 4 shows the SPD for each channel operated at the ambient temperature $T_a$ of 10 $^{o}$C with the DC drive current $I_{DC}$ of 350 mA, respectively. An adequate layout of LED pixel arrangement and first-order design is helpful to deliver a uniform illumination upon the test Macbeth color checker [13].

To evaluate the performance of the combinations in SPD, an application-oriented merit function should be defined. In this case we introduce a user-defined function, based on the weighted sum method, with the figures of merit luminous efficiency (LE) and color quality scale (CQS) [14].

$$f = w \times CQS + (1 - w) \times LE$$
$$\text{subject to the constrain: weight } w \in [0,1] \tag{3}$$

where the weight factor, w, is used to provide a freedom to determine the operational mode. When $w = 0$, the system is carried out in high efficiency mode, the objective function is entirely attributed to the efficiency consideration. The other extreme case ($w = 1$) would be high quality mode.

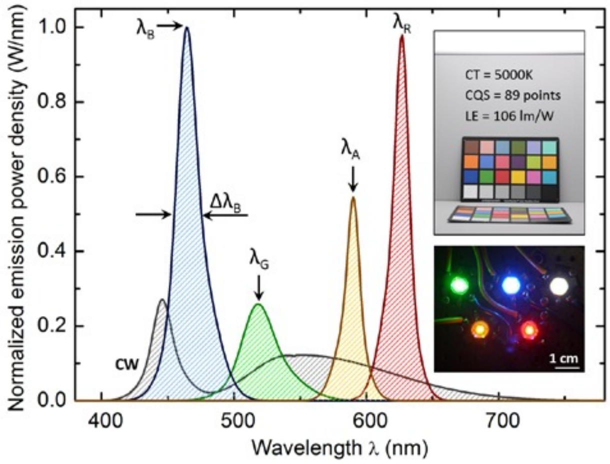


Figure 4 The power spectra of red ($\lambda_R$: 625nm, $\Delta\lambda_R$: 20nm), green ($\lambda_G$: 523nm, $\Delta\lambda_G$: 33nm), blue ($\lambda_B$: 465nm, $\Delta\lambda_B$: 25nm), amber ($\lambda_A$: 587nm, $\Delta\lambda_A$: 18nm) and cool-white LEDs at $T_a$ of 10 °C with $I_{DC}$ of 350 mA. The upper right figure shows a real-field test designed for color temperature (CT) of 5000K and the lower right one shows the utilized LEDs attached on the temperature controllable fixture respectively.

The first validation is conducted by examining the temperature dependence of spectra under four color temperatures: CT = 3200K, 4600K, 6200K, and 7400K, respectively. The system is operated under a specific value of the ambient temperature, $T_a$ = 50°C. The results are reported in Figure 5(a), where the illumination conditions fulfill the requirements of high luminance level (100 lm), negligible color deviation (Δxy < 0.01) and high quality (CQS > 85 points) with possibly highest luminous efficiency (LE). If we change the ambient temperature without compensation, the lighting performance would dramatically shift due to the thermal effects. The reason can be explained by Figure 5(b). When the ambient temperature $T_a$ increases to 100 °C, luminous efficiencies (LEs) of amber and red LED suffer from 23% and 46% decreases of those at 10 °C, respectively. The results can be attributed to two reasons: (1) In viewpoint of spectral characteristics, at high ambient temperature $T_a$, the SPDs of amber and red color would shift to longer wavelength, result in the decreases of luminous efficiency [15]. (2) In terms of material, for the AlInGaP-based LEDs, due to the carrier overflow by increased ambient temperature, the luminous efficiency would be reduced accordingly [16]. In order to compensate the operational shift by thermal effects, the proposed scheme is then included.

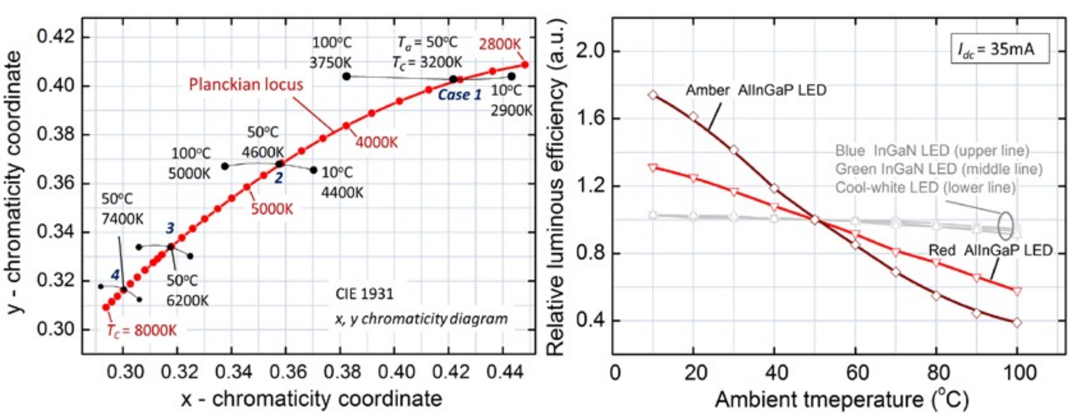


Figure 5 (a) The temperature dependence of spectra designed for CT = 3200K, 4600K, 6200K, and 7400K at $T_a$ = 50 °C. (b) The temperature dependence of LE for pentachromatic LEDs.

The optimized outcome is shown in Figure 6. The contour map of possibly highest luminous efficiency (LE) subject to predefined requirements (CQS > 85 points, high luminance level 100 lm and negligible color deviation Δxy < 0.01 ). As the ambient temperature increases, it can be observed that the efficiency will deteriorate and move toward the left-up corner. The best performance (LE > 130 lm/W) lies in a narrow region about CT = 4000-6500K associated with self-evident low ambient temperature ($T_a$ =10 $^o$C ~ 20 $^o$C). If the LE = 100 lm/W is settled as the minimum requirement, a full operable range for $T_a$ is workable only exists in high color temperature CT > 5200K.

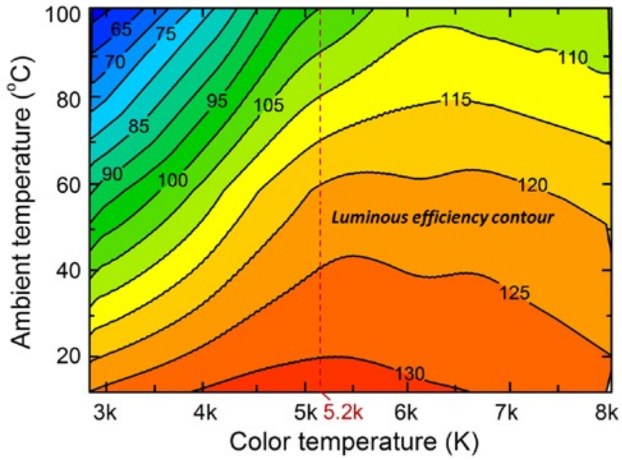


Figure 6 The *LE* contour of the pentachromatic LEDs cluster is performed under the predefined requirements (*CQS* > 85 points, lighting level =100 *lm* and Δ*xy* < 0.01). When the *LE* = 100 *lm*/watt is selected as the minimum efficiency boundary, a full operation range for ambient temperature can be obtained for *CT* > 5200K.

## 4. CONCLUSION

A complete high power LEDs mixing scheme has been proposed in consideration of the spectral formalism and the optimization methodology. The phosphor-converted white light can be approximated by simply decomposing the spectrum into two double-Gaussian models developed from single-color spectrum. In the optimization process, a design procedure analogous to the conventional lens design process has been proposed. The algorithm enables the users to easily determine the optimal LEDs set to meet the requirements such as light efficiency, color quality, or other figures of merit over a wide range of color temperature. In order to implement the proposed scheme, a pentachromatic high power cluster is devised. The limitation in operation window at high $T_a$ and low $T_c$ is mainly due to the dramatically deteriorations in luminous efficiency of amber and red light sources, which could be improved by replacing single emitter to two or more ones to share the total emitting power and reduce the thermal effect induced by drive current. However, the cluster provides a full operable range in ambient temperature when $T_c$ > 5200K by using the proposed scheme, which makes it feasible to provide a high quality smart lighting system that can be efficiently operated with an extended operable range.

## REFERENCES

[1] Schubert, E. F., Kim, J. K., Luo, H. and Xi, J.-Q., “Solid-state lighting – A benevolent technology,” Rep Prog. Phys. 69, 3069-3098 (2006).
[2] Pimputkar, S., Speck, J. S., DenBaars, S. P. and Nakamura, S., “Prospects for LED lighting,” Nat. Photonics 3(4), 180–182 (2009).
[3] Schubert, E. F. and Kim, J. K., “Solid-state light sources getting smart,” Science 308(5726), 1274–1278 (2005).
[4] J. K. Kim and E. F. Schubert, "Transcending the replacement paradigm of solid-state lighting," Opt. Express 16, 21835–21842 (2008).
[5] Žukauskas, A., Vaicekauskas, R. and Shur, M. S., “Solid-state lamps with optimized color saturation ability,” Opt. Express 18, 2287-2295 (2010).
[6] He, G. and Zheng, L., “White-light LED clusters with high color rendering,” Opt. Lett. 35, 2955–2957 (2010).

[7] Gonzalez, R. C. and Wood, R. E., [Digital Image Processing], Prentice Hall, (2007).
[8] Betti, S., Marchis, G. D. and Iannone, E., [Coherent Optical Communications Systems], Wiley, (1995).
[9] Chou, H. Y. and Yang, T. H., "Dependence of emission spectra of LEDs upon junction temperature and driving current," J. Light Visual Environ. 32, 183–186 (2008).
[10] Reifegerste, F. and Lienig, J., "Modeling of the temperature and current dependence of LED spectra," J. Light Visual Environ. 32, 288–294 (2008).
[11] Smith, W. J., [Modern optical engineerin], McGraw-Hill Professional, (2000).
[12] Kingslake, R., [Lens design fundamentals], Academic Press, (1978).
[13] Moreno, I., Avendaño-Alejo, M. and Tzonchev, R. I., "Designing light-emitting diode arrays for uniform near-field irradiance," Appl. Opt. 45, 2265–2272 (2006).
[14] Wood, M., "CRI and the Color Quality Scale, Part 2" Protocol Spring 15(2), 14–18 (2010).
[15] Xi, Y. and Schubert, E.F., "Junction-temperature measurement in GaN ultraviolet light-emitting diodes using diode forward voltage method," Appl. Phys. Lett. 85(12), 2163–2165 (2004).
[16] Mukai, T., Yamada M. and Nakamura, S., "Characteristics of InGaN-Based UV/Blue/Green/Amber/Red Light-Emitting Diodes," Jpn. J. Appl. Phys. 38, 3976–3981 (1999).